Towards superior van der Waals density functionals for molecular crystals

Dmitry V. Fedorov,^{1,*} Nikita E. Rybin,^{1,2} Mikhail A. Averyanov,^{1,3} Alexander V. Shapeev,^{1,2} Artem R. Oganov,¹ and Carlo Nervi^{1,†}

Ubiquitous van der Waals (vdW) interactions play a subtle yet crucial role in determining the precise atomic arrangements in solids, particularly in molecular crystals where these weak forces are the primary link between constituent building blocks. Within density functional (DF) theory, the most natural approach for addressing vdW forces is the use of vdW-inclusive density functionals. Through a detailed analysis of the underlying formalism, we have developed a computational scheme that combines vdW functionals of type DF1 and DF2 and serves as a well optimizable tool to improve the theoretical description and prediction of molecular crystals and other sparse materials. The proof of principle is demonstrated by our consideration of the molecular crystals from the X23 dataset.

Accurate yet computationally affordable theoretical descriptions of molecular crystals (MCs) are highly desirable in both established and emerging fields, such as the design of high-energy materials, pharmaceutical compounds, and molecular solids with tailored properties [1]. The structure and stability of these materials are often governed by weak intermolecular interactions. Although constituting only a small fraction of the total electronic energy, they are decisive in determining the final crystalline arrangement through their significant forces [2–5].

Among them, the omnipresent van der Waals (vdW) interaction is a subtle quantum-mechanical phenomenon related to electrodynamically correlated charge fluctuations at different atoms in molecular systems and materials [6–8]. Due to their long-range character, it is not so trivial to describe them within the framework of density functional theory (DFT). Among different approaches to tackle vdW forces within first-principles calculations, the vdW density functionals (DFs) attract a special attention, since they are naturally built within the DFT formalism as well as strongly related to the robust randomphase approximation (RPA) [9]. The great progress in the corresponding field of research has been reviewed in Refs. [10, 11]. In addition, an elucidating interpretation of vdW-DFs was given by Hyldgaard et al. [12], who comprehensively discussed the connection of vdW-DFs and the RPA intimately linked to the many-body dispersion (MBD) method possessing high accuracy [13–16].

In this Letter, we provide readers with a concise yet fairly complete description of the related formalism and present an optimization procedure to design vdW-DFs outperforming the existing vdW approaches in describing both, unit cell volumes and lattice energies, as demonstrated for the MCs from the X23 dataset [17–20]. The proposed approach is a good alternative to the MBD method, delivering comparable accuracy to the latter yet being significantly less demanding (especially, for MCs).

The concept of nonlocal vdW-DFs [21] has been developed in the framework of the DFT employing local density approximation (LDA) and generalized gradient

approximation (GGA), through representing the total exchange-correlation functional by the sum [10, 11]

$$E_{\rm xc}^{\rm vdW-DF}[n] = E_{\rm xc}^{0}[n] + E_{c}^{\rm nl}[n] ,$$
 (1)

where the semilocal (outer) functional

$$E_{\rm xc}^0[n] = E_{\rm x}^{\rm GGA}[n] + E_{\rm c}^{\rm LDA}[n] = \int d\mathbf{r} \, n(\mathbf{r}) \, \mathcal{E}_{\rm xc}^0(\mathbf{r}) \quad (2)$$

consists of LDA correlation and GGA exchange energy: $\mathcal{E}_{xc}^{0}(\mathbf{r}) = \mathcal{E}_{x}^{GGA}(\mathbf{r}) + \mathcal{E}_{c}^{LDA}(\mathbf{r})$. In practice, the correlation is treated within the Perdew-Burke-Ernzerhof (PBE) approach [22], whereas a various choice of the GGA exchange leads to a number of different vdW-DFs [10, 11]. Another reason for their distinction lies in the nonlocal correlation energy E_{c}^{nl} , which we discuss in detail below. The explicit separation of nonlocal correlation from its LDA counterpart is made to avoid a double counting. However, E_{xc}^{0} by itself normally delivers a typical GGA description since gradient corrections are more important for exchange than for correlation [12, 23, 24]. That is why the correlation energy in its PBE form [22] is usually employed for $E_{xc}^{0}[n]$ to perform calculations with vdW-DFs.

The coupling of plasmon poles corresponding to the electronic structure obtained by means of the outer functional delivers the nonlocal correlation energy [25]

$$E_c^{\text{nl}}[n] = \frac{1}{2} \iint d\mathbf{r} \, d\mathbf{r}' n(\mathbf{r}) \phi(\mathbf{r}, \mathbf{r}') n(\mathbf{r}') , \qquad (3)$$

where the kernel $\phi(\mathbf{r}, \mathbf{r}') = \phi[d(\mathbf{r}, \mathbf{r}'), d'(\mathbf{r}, \mathbf{r}')]$ depends on the coordinates through the scaled separations [26]

$$d(\mathbf{r}, \mathbf{r}') = |\mathbf{r} - \mathbf{r}'|q_0(\mathbf{r}), \quad d'(\mathbf{r}, \mathbf{r}') = |\mathbf{r} - \mathbf{r}'|q_0(\mathbf{r}').$$
 (4)

Here, $q_0(\mathbf{r}) = k_{\rm F}(\mathbf{r}) f_x^{\rm in}(s) - (\frac{4\pi}{3}) \mathcal{E}_c^{\rm LDA}(\mathbf{r})$ [25] equal to [10]

$$q_0(\mathbf{r}) = \frac{k_{\rm F}(\mathbf{r})}{\mathcal{E}_x^{\rm LDA}(\mathbf{r})} \left[\mathcal{E}_x^{\rm LDA}(\mathbf{r}) f_x^{\rm in}(s) + \mathcal{E}_c^{\rm LDA}(\mathbf{r}) \right] , \quad (5)$$

with the scaled gradient $s \equiv s(\mathbf{r}) = |\nabla n(\mathbf{r})|/2n(\mathbf{r})k_{\mathrm{F}}(\mathbf{r})$ of the electron density $n(\mathbf{r})$ and $k_{\mathrm{F}}(\mathbf{r}) = [3\pi^2 n(\mathbf{r})]^{1/3}$. In

Skolkovo Institute of Science and Technology, Bolshoy Boulevard 30, 121205 Moscow, Russia
Digital Materials LLC, Kutuzovskaya street 4A, 143001, Odintsovo, Russia
Mendeleev University of Chemical Technology of Russia, Miusskaya Square 9, 125047 Moscow

addition, $\mathcal{E}_x^{\text{LDA}}(\mathbf{r}) = -(3/4\pi)k_{\text{F}}(\mathbf{r})$ and $\mathcal{E}_c^{\text{LDA}}(\mathbf{r})$ corresponds to the (local) correlation of the outer functional. Furthermore, $q_o(\mathbf{r})$ contains the enhancement factor

$$f_x^{\text{in}}(s) = 1 - (Z_{ab}/9)s^2 \tag{6}$$

related to the exchange gradient. Originally, the (inner) enhancement factor was taken following an analysis for screened exchange of Langreth and Vosko [27] who obtained $Z_{ab} = -0.8491$, from a gradient expansion for the slowly varying electron gas. This model is assumed to work well for solids with relatively homogeneous electron distributions. The above value has been employed for vdW-DF1 [28] but modified later for vdW-DF2 [29] to $Z_{ab} = -1.8867$, stemming from a large-N asymptotic analysis [30, 31], where N is the number of electrons. The modification has been aimed to better describe atoms and molecules [32]. In addition to Z_{ab} , the two vdW-DFs employ different functional forms for their outer functional. The exchange-correlation energy density in Eq. (5),

$$\mathcal{E}_{xc}^{\text{in}}(\mathbf{r}) = \mathcal{E}_{x}^{\text{LDA}}(\mathbf{r}) f_{x}^{\text{in}}(s) + \mathcal{E}_{c}^{\text{LDA}}(\mathbf{r}) , \qquad (7)$$

is related to the semilocal inner functional

$$E_{\rm xc}^{\rm in}[n] = \int d\mathbf{r} \, n(\mathbf{r}) \, \mathcal{E}_{\rm xc}^{\rm in}(\mathbf{r}) \;, \tag{8}$$

which differs from the outer functional by [11]

$$\delta E_{\rm x}^0[n] = E_{\rm xc}^0[n] - E_{\rm xc}^{\rm in}[n] \ .$$
 (9)

The difference reflects a more rapid increase of $\mathcal{E}_{xc}^{in}(\mathbf{r})$ at large values of $s(\mathbf{r})$ in comparison to $\mathcal{E}_{xc}^{0}(\mathbf{r})$, which ensures divergence of the scaled separations tuning out E_c^{nl} [26], to avoid spurious contributions from low-density regions [12]. For each type of vdW-DFs, δE_x^0 is determined by the value of Z_{ab} in $f_x^{in}(s)$ entering $\mathcal{E}_{xc}^{in}(\mathbf{r})$ of Eq. (7) and by choice of outer exchange-energy density

$$\mathcal{E}_x^{\text{GGA}}(\mathbf{r}) = \mathcal{E}_x^{\text{LDA}}(\mathbf{r}) F_x(s) , \qquad (10)$$

defined by the related enhancement factor $F_x(s)$ [10].

Thus, various vdW-DFs can be distinguished by the choice of $F_x(s)$ together with the different parametrization of $f_x^{\rm in}(s)$ encoded in the value of Z_{ab} . The authors of Ref. [10] encouraged the use of a standard nomenclature vdW-DF- E_x with E_x referring to the exchange functional. Here, we follow their suggestion but make an extension of the nomenclature to specify also the magnitude of Z_{ab} employed in a scheme: vdW-DF- E_x - Z_{ab} .

To consistently treat exchange energy between outer and inner functionals, in Ref. [26] the functional vdW-DF-cx was introduced, where the enhancement factor

$$F_x^{\text{LV-PW86R}}(s) = \frac{f_x^{\text{in}}(s)}{1+\alpha s^6} + \left(\frac{\alpha s^6}{\beta + \alpha s^6}\right) F_x^{\text{PW86R}}(s) \quad (11)$$

splines the Langreth-Vosko gradient expansion [27] of Eq. (6) with the PW86R [33] enhancement factor [34, 35]:

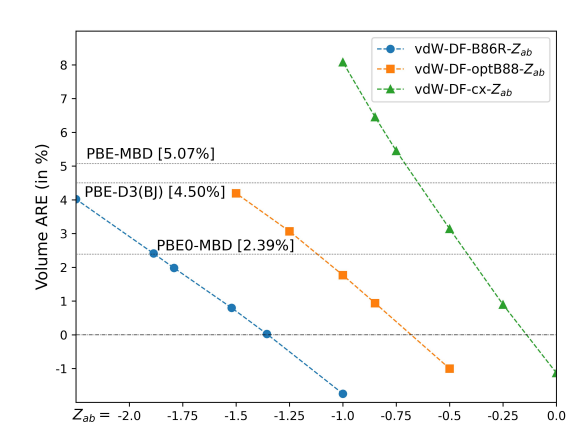


FIG. 1: The average relative error for the unit cell volume of the X23 crystals for the considered vdW-DF-optB88- Z_{ab} , vdW-DF-B86R- Z_{ab} , and vdW-DF-cx- Z_{ab} functionals. As the reference data, the cell volumes $V_{\rm el}^{\rm ref}$ from Ref. [20] are taken.

 $F_x^{\text{PW86R}}(s) = (1 + as^2 + bs^4 + cs^6)^{1/15}, \ a = 1.851, b = 17.33, \text{ and } c = 0.163.$ The spline procedure, where $\alpha = 0.02178$ and $\beta = 1.15$ [26], ensures consistent exchange (cx) treatment (for small values of s). Similar to vdW-DF1 functionals, vdW-DF-cx uses $Z_{ab} = -0.8491$.

In addition, we employ optB88-vdW(-DF1) [36] and rev-vdW-DF2 (also known as vdW-DF-B86R) [37], which are vdW-DF-optB88-0.8491 and vdW-DF-B86R-1.8867 within our nomenclature. These functionals, corresponding to DF1 and DF2 types [10, 11], respectively, deliver relatively accurate results for MCs, in contrast to vdW-DF3 functionals showing poor performance for such systems [38]. For the two functionals, the outer enhancement factors are formally the same as the ones of the related B88 and B86b functionals and differ from their counterparts just by a couple of (optimized) parameters. The vdW-DF-optB88 enhancement factor reads [36, 39]

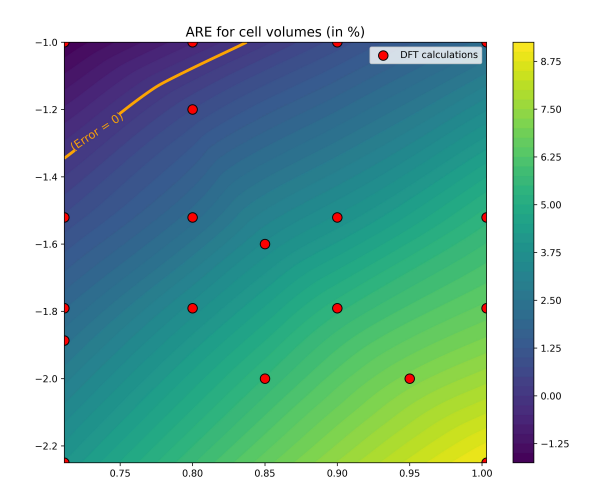
$$F_x^{\text{optB88}}(s) = 1 + \mu s^2 / [1 + \beta s \arcsin(cs)],$$
 (12)

where $\mu = 0.22$, $\beta = \mu/1.2$, and $c = 2(6\pi^2)^{1/3}$. This enhancement factor stems from the original B88 functional of Becke [39], with $\mu = 0.2743$ and $\beta = 9\mu/4\pi$. The vdW-DF-B86R enhancement factor is given by [37, 40]

$$F_x^{\text{B86R}}(s) = 1 + \frac{\mu s^2}{(1 + \mu s^2/\kappa)^{4/5}}$$
, (13)

where $\mu = 10/81$ and $\kappa = 0.7114$. The functional form of Eq. (13) is also valid for its original counterpart from the B86b functional [40]. The corresponding parameters $\mu = 0.2449$ and $\kappa = 0.5757$ [35] can be obtained from $\beta = 0.00375$ and $\gamma = 0.007$ of Becke [40] through the following relations: $\mu = \beta(16\pi/3)(6\pi^2)^{1/3} = 4\gamma\kappa(6\pi^2)^{2/3}$ [41].

The details of our DFT calculations performed by the Vienna Ab Initio Simulation Package (VASP) [42–45] are given in the Supplemental Material (SM) [46]. We optimize the choice of Z_{ab} restricted by us to be between its



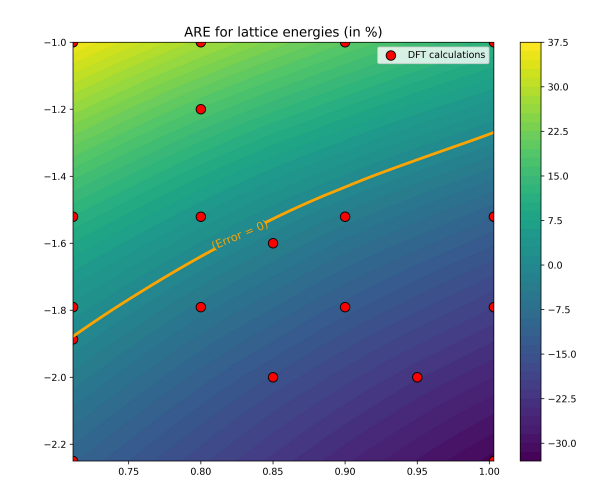


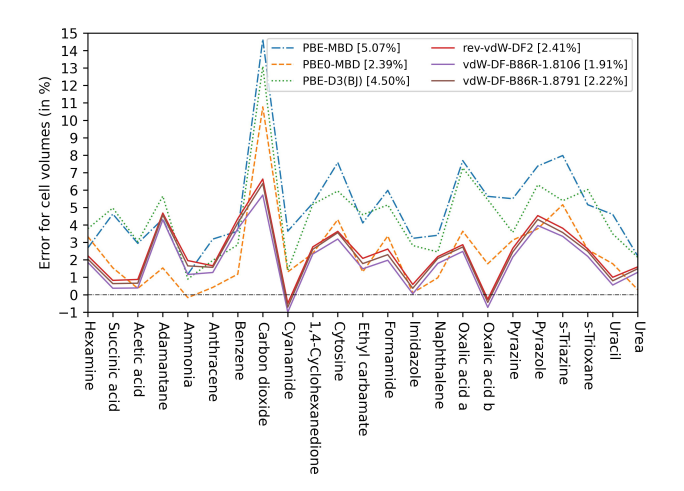
FIG. 2: The two-dimensional map of the average errors for unit cell volumes and lattice energies of the X23 molecular crystals. The results obtained for original points (labeled with red dots) are interpolated to $0.7114 < \kappa < 1.0031$ and $-2.25 < Z_{ab} < -1$.

vdW-DF1 and vdW-DF2 counterparts, as defining the range of reasonable values for this parameter, according to the aforementioned limits for the electron density. It is natural to consider MCs as corresponding to a certain intermediate case with a related in-between value of Z_{ab} . We also tune the parameter κ in Eq. (13). The aforementioned original parameters β and γ of Becke [40] were obtained by fitting to noble gas atoms. The values give $\beta/\gamma^{4/5} = 0.20$, whereas the theoretical large-gradient model gives $\beta/\gamma^{4/5} = 0.27$ [40]. The latter ratio delivers $\kappa = 1.0031$, for $F_x^{\text{B86R}}(s)$, if the parameter μ is fixed to its theoretical value of 10/81. The obtained parameter set is very close to the one of $F_x^{\text{optB86b}}(s) = 1 + \mu s^2 / (1 + \mu s^2)^{4/5}$, with $\mu = 10/81$ and $\kappa = 1$, which is known to deliver an accuracy similar to $F_x^{\text{optB88}}(s)$ [47]. We change κ in Eq. (13) between 0.7114 and 1.0031, as a resonable range for its possible values. In addition, for all the three considered functionals, the parameter Z_{ab} is tuned in our optimization scheme. Below we show that the designed functional of the proposed vdW-DF1.5 type delivers accurate results for cell volumes and lattice energies of MCs from the X23 dataset [17–20]. For these quantities, we employ the X23b reference values [20], where phonon contributions (thermal and zero-point energy effects) are "removed" from experimental data. This comparison ensures the most reasonable benchmark between different (pure electronic) approaches considered here. Choosing more accurate reference data (once available in the future) could change a detailed picture, but the proposed optimization procedure as well as the general arguments for possible improvements of vdW-DFs stay in force.

First, let us consider unit cell volumes of the MCs from the X23 dataset obtained by means of the three distinct vdW-DFs with varying Z_{ab} . As the reference data, we use the volumes corresponding to the electronic energy surface $V_{\rm el}^{\rm ref}$ derived in Ref. [20] by extracting the phonon contributions from the experimental data.

By this way we explore different computational schemes solely with respect to their quality in describing longrange electronic correlations. Figure 1 shows a monotonic (almost linear) behavior of $V_{\rm err} = (V_{\rm calc} - V_{\rm el}^{\rm ref})/V_{\rm el}^{\rm ref}$, where $V_{\rm calc}$ denotes calculated values. As extended systems, MCs are significantly influenced by the electrodynamic screening [14, 49], which can remarkably reduce vdW interactions [16]. Increasing the magnitude of Z_{ab} leads to decreasing the attractive forces and consequently to larger cell volumes calculated with vdW-DFs. The corresponding weaker attraction in the asymptotic region of vdW-DF2 in comparison to vdW-DF1 was mentioned in Ref. [29]. From Fig. 1, the best performance is achieved with vdW-DF-B86R-1.356, vdW-DF-optB88-0.678, and vdW-DF-cx-0.139 delivering the vanishing average relative error (ARE). However, the range of most reasonable values for Z_{ab} is between $Z_{ab} = -0.8491$ and $Z_{ab} = -1.8867$ derived [50], respectively, for solids [27] and atoms/molecules [29] as two limits for condensed matter phases. With $Z_{ab} = -1.356$ in between of the two above values, the best justified choice corresponds to vdW-DF-B86R-1.356, if one focuses on the cell volumes.

From the X23b dataset [20] we also employ the lattice energy, as a good benchmark quantity depending only on the electronic and nuclear-repulsion energies [51]. Unfortunately, the above vdW-DF-B86R-1.356 scheme delivers the energy ARE of about 20% instead of a few percent typical for other methods (see the right panel of Fig. 3). To find a compromise in describing both quantities simultaneously, we perform an extended search for an optimized computational scheme, also varying the parameter κ from Eq. (13) between 0.7114 and 1.0031, according to our discussion above. Figure 2 shows the dependence of the AREs on the values of κ and Z_{ab} . For both, the volumes and energies separately, there is a continuous curve related to a set of $\{\kappa, Z_{ab}\}$ where the ARE is vanishing. However, the two curves go almost parallel to each other



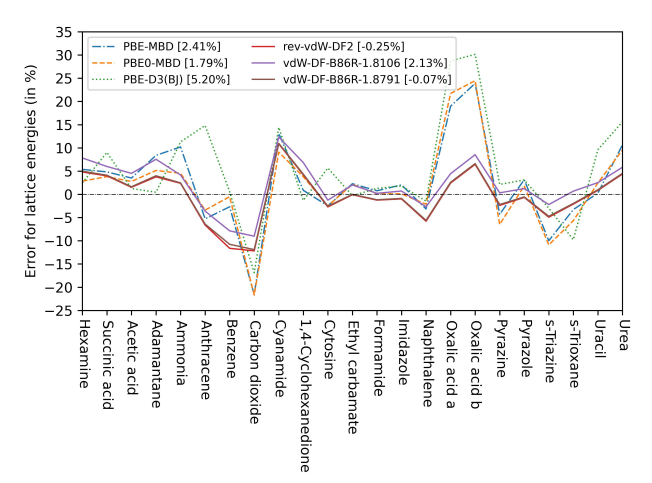


FIG. 3: The relative error for cell volumes (left) and lattice energies (right) of the X23 molecular crystals calculated by PBE-MBD [48], PBE0-MBD [48], PBE-D3 (with the Becke-Johnson damping function) [48], rev-vdW-DF2 (identical to vdW-DF-B86R-1.8867 in our notations), vdW-DF-B86R-1.8106, and vdW-DF-B86R-1.8791 functionals. As the reference data, the cell volumes $V_{\rm el}^{\rm ref}$ and the lattice energies $E_{\rm latt}^{\rm ref,exp}$ from Ref. [20] are employed, as fairly corresponding to pure electronic results.

without crossing. This finding reflects the general problem of all vdW approaches, which are not capable to deliver vanishing ARE for both, volume and energy at the same time. The considered functional is quite useful for further potential improvement of vdW-DFs. As follows from Fig. 2, the functional form of $F_x^{\rm B86R}(s)$ needs to be modified, in order to achieve its excellent performance. The opportunity to play (just) with two physically transparent parameters makes the chosen scheme suitable for intensive tests. With reaching a progress for this functional, one could also modify $F_x(s)$ belonging to others (for their variety, see Fig. 11 in Ref. [10]), in order to develop a new class of superior vdW-DFs. To achieve such an ambitious goal, machine learning approaches (including symbolic regression) can play an important role.

Using the results from Fig. 2 (see the SM [46] for details), vdW-DF-B86R-1.8106 and vdW-DF-B86R-1.8791 are identified as two good optimizations of rev-vdW-DF2. Their performance is demonstrated by Fig. 3 via comparison to the results of Ref. [48] obtained by MBD [13–16] and D3 [52, 53] (with the Becke-Johnson damping function [54–58]) methods. For consistency with vdW-DFs, the PBE functional [22] has been employed for all approaches. In addition, the results [48] of the PBE0-MBD method, an assumed gold standard for MCs, are also presented. As shown by Fig. 3, the vdW-DF-B86R-1.8791 scheme outperforms other approaches. In a similar way, the vdW-DF-B86R-1.8106 scheme delivers the accuracy comparable to the PBE0-MBD method. The corresponding screening parameter is very close to $Z_{ab} = -1.79075$, as derived from the large-N asymptotic analysis [50]. The corresponding vdW-DF-B86R-1.79075 delivers the volume and energy ARE of 1.98% and 2.63%, respectively, again comparable to the PBE0-MBD results. Thus, the correction of Z_{ab} for DF2 functionals from its widely used

empirical value to the actually derived counterpart seems to be the right modification for vdW-DFs, serving as another reasonable constraint. Although both of our optimized schemes employ the standard value of $\kappa=0.7114$ from Eq. (13), the option to vary this parameter paves the way for further improvements within the B86R family of vdW-DFs. We foresee such an opportunity based on our detailed analysis, which is discussed in the SM [46].

We subscribe to the authors of Ref. [10] for their belief in the replacement of dispersion-corrected DFT by nonlocal vdW-DFs. Based on our results, further intensive studies in this direction are anticipated, in order to develop advanced vdW-DFs capable to cope with sparse materials, where vdW forces can significantly act through important low-density regions [11]. The relevant materials are not restricted to molecular crystals but belong to vast classes of systems such as layered materials, polymers, and covalent or metal-organic frameworks.

In summary, we propose vdW-DF1.5 functionals, as combination of already existing DF1 and DF2 types, with a corresponding procedure of their optimization for any class of materials. The proof of principle is demonstrated on the X23 dataset of molecular crystals, for which our vdW-DF-B86R-1.8791 scheme outperforms the results of other computational vdW approaches in both, unit cell volumes and lattice energies. Our work delivers a helpful insight into the considered problem as well as useful hints to further improve van der Waals density functionals, for a natural and efficient way of tackling the subtle longrange correlations within the density functional theory.

The work was supported by the grant for research centers in the field of AI provided by the Ministry of Economic Development of the Russian Federation in accordance with the agreement 000000C313925P4F0002 and the agreement with Skoltech №139-10-2025-033.

- * Electronic address: Dm.Fedorov@skoltech.ru
- † Electronic address: C.Nervi@skoltech.ru
- [1] G. K. Kole, R. Medishetty, M. H. Mir, J. K. Zaręba, M. Hasegawa, L. R. MacGillivray, S. Konar, and J. W. Steed, Cryst. Growth Des. 25, 1949 (2025).
- [2] C.-S. Liu, G. Pilania, C. Wang, and R. Ramprasad, J. Phys. Chem. A 116, 9347 (2012).
- [3] A. M. Reilly and A. Tkatchenko, Chemical Science 6, 3289 (2015).
- [4] S. Kawai, A. S. Foster, T. Björkman, S. Nowakowska, F. F. C. Jonas Björk, L. H. Gade, T. A. Jung, and E. Meyer, Nature Communications 7, 11559 (2016).
- [5] L. L. Presti, CrystEngComm **20**, 5976 (2018).
- [6] A. J. Stone, The Theory of Intermolecular Forces (Oxford University Press, 1996).
- [7] V. A. Parsegian, Van der Waals forces: A Handbook for Biologists, Chemists, Engineers and Physicists (Cambridge University Press, 2005).
- [8] I. G. Kaplan, Intermolecular Interactions: Physical Picture, Computational Methods and Model Potentials (New York: Wiley, 2006).
- [9] X. Ren, P. Rinke, C. Joas, and M. Scheffler, J. Mater. Sci. 47, 7447 (2012).
- [10] K. Berland, V. R. Cooper, K. Lee, E. Schröder, T. Thonhauser, P. Hyldgaard, and B. I. Lundqvist, Rep. Prog. Phys. 78, 066501 (2015).
- [11] P. Hyldgaard, Y. Jiao, and V. Shukla, J. Phys.: Condens. Matter 32, 393001 (2020).
- [12] P. Hyldgaard, K. Berland, and E. Schröder, Phys. Rev. B 90, 075148 (2014).
- [13] A. Tkatchenko, R. A. DiStasio, Jr., R. Car, and M. Scheffler, Phys. Rev. Lett. 108, 236402 (2012).
- [14] R. A. DiStasio, Jr., V. V. Gobre, and A. Tkatchenko, J. Phys.: Condens. Matter 26, 213202 (2014).
- [15] A. Tkatchenko, R. A. DiStasio, Jr., R. Car, and M. Scheffler, J. Chem. Phys. 140, 18A508 (2014).
- [16] D. Massa, A. Ambrosetti, and P. L. Silvestrelli, J. Chem. Phys. 154, 224115 (2021).
- [17] A. O. de-la Roza and E. R. Johnson, J. Chem. Phys. 137, 054103 (2012).
- [18] A. M. Reilly and A. Tkatchenko, J. Chem. Phys. 139, 024705 (2013).
- [19] M. Mortazavi, J. G. Brandenburg, R. J. Maurer, and A. Tkatchenko, J. Phys. Chem. Lett. 9, 399 (2018).
- [20] G. A. Dolgonos, J. Hoja, and A. D. Boese, Phys. Chem. Chem. Phys. 21, 24333 (2019).
- [21] We discuss the formalism related to the general-geometry vdW-DFs, which is partially valid for their (original) layered-geometry counterpart (vdW-DF0). The detailed comparison of the two vdW-branches is given in Ref. 10.
- [22] J. P. Perdew, K. Burke, and M. Ernzerhof, Phys. Rev. Lett. 77, 3865 (1996).
- [23] J. P. Perdew, L. A. Constantin, E. Sagvolden, and K. Burke, Phys. Rev. Lett. 97, 223002 (2006).
- [24] L. A. Constantin, J. P. Perdew, and J. M. Pitarke, Phys. Rev. B 79, 075126 (2009).
- [25] T. Thonhauser, V. R. Cooper, S. Li, A. Puzder, P. Hyldgaard, and D. C. Langreth, Phys. Rev. B 76, 125112 (2007).
- [26] K. Berland and P. Hyldgaard, Phys. Rev. B 89, 035412 (2014).

- [27] D. C. Langreth and S. H. Vosko, Adv. Quant. Chem. 21, 175 (1990).
- [28] M. Dion, H. Rydberg, E. Schröder, D. C. Langreth, and B. I. Lundqvist, Phys. Rev. Lett. 92, 246401 (2004).
- [29] K. Lee, Éamonn D. Murray, L. Kong, B. I. Lundqvist, and D. C. Langreth, Phys. Rev. B 82, 081101(R) (2010).
- [30] J. Schwinger, Phys. Rev. A 22, 1827 (1980).
- [31] J. Schwinger, Phys. Rev. A **24**, 2353 (1981).
- [32] P. Elliott and K. Burke, Can. J. Chem. 87, 1485 (2009).
- [33] In contrast to the authors of Ref. 26 who used the abbreviation PW86r within the discussion of their vdW-DF-cx functional, we employ the original abbreviation PW86R used by its inventors in Ref. 29 as well as by Hamada [37].
- [34] J. P. Perdew and Y. Wang, Phys. Rev. B 33, 8800 (1986).
- [35] Éamonn D. Murray, K. Lee, and D. C. Langreth, J. Chem. Theory Comput. 5, 2754 (2009).
- [36] J. Klimeš, D. R. Bowler, and A. Michaelides, J. Phys.: Condens. Matter 22, 022201 (2010).
- [37] I. Hamada, Phys. Rev. B 89, 121103 (2014).
- [38] D. Chakraborty, K. Berland, and T. Thonhauser, J. Chem. Theory Comput. 16, 5893 (2020).
- [39] A. D. Becke, Phys. Rev. A 38, 3098 (1988).
- [40] A. D. Becke, J. Chem. Phys. 85, 7184 (1986).
- [41] The relation between μ and β given within Ref. [26] of the paper by Lee *et al.* [29] needs the following correction: $\mu = (16\pi/3)(3\pi^2)^{1/3}\beta \rightarrow \mu = (16\pi/3)(6\pi^2)^{1/3}\beta$.
- [42] G. Kresse and J. Hafner, Phys. Rev. B 47, 558 (1993).
- [43] G. Kresse and J. Hafner, Phys. Rev. B 49, 14251 (1994).
- [44] G. Kresse and J. Furthmüller, Phys. Rev. B 54, 11169 (1996).
- [45] G. Kresse and J. Furthmüller, Computational Materials Science 6, 15 (1996).
- [46] See Supplemental Material at http://link.aps.org/supplemental/... for computational details and an extended discussion of the results.
- [47] J. Klimeš, D. R. Bowler, and A. Michaelides, Phys. Rev. B 83, 195131 (2011).
- [48] O. A. Loboda, G. A. Dolgonos, and A. D. Boese, J. Chem. Phys. 149, 124104 (2018).
- [49] B. Schatschneider, J.-J. Liang, A. M. Reilly, N. Marom, G.-X. Zhang, and A. Tkatchenko, Phys. Rev. B 87, 060104(R) (2013).
- [50] The actual value for atoms/molecules, which can be derived from the related asymptotic analysis [30–32], reads $Z_{ab} = -1.79075$ instead of $Z_{ab} = -1.8867$ commonly employed for vdW-DF2 by convention [29]. The correction factor of about 0.949 is the ratio of derived 2.109 [32] and empirical 2.222 [39] values for $Z_{ab}^{\text{DF2}}/Z_{ab}^{\text{DF1}}$, where $Z_{ab}^{\text{DF1}} = -0.8491$. The empirical value was chosen by the authors of Ref. 29 for their first vdW-DF2 functional and then became widely used for the DF2 type of vdW-DFs.
- [51] J. Hoja, A. M. Reilly, and A. Tkatchenko, WIREs Comput. Mol. Sci. 7, e1294 (2017).
- [52] S. Grimme, J. Antony, S. Ehrlich, and H. Krieg, J. Chem. Phys. 132, 154104 (2010).
- [53] S. Grimme, WIREs Comput. Mol. Sci. 1, 211 (2011).
- [54] A. D. Becke and E. R. Johnson, J. Chem. Phys. 123, 154101 (2005).
- [55] E. R. Johnson and A. D. Becke, J. Chem. Phys. 123, 024101 (2005).
- [56] E. R. Johnson and A. D. Becke, J. Chem. Phys. 124, 174104 (2006).
- [57] S. Grimme, S. Ehrlich, and L. Goerigk, J. Comput.

Chem. **32**, 1456 (2011). [58] L. Goerigk, A. Hansen, C. Bauer, S. Ehrlich, A. Najibi, and S. Grimme, Phys. Chem. Chem. Phys. **19**, 32184 (2017).